

Response to referees' comments on manuscript "Rate enhancement in collisions of sulfuric acid molecules due to long-range intermolecular forces"

Dear Editor,

We thank the two anonymous referees for the favorable review of our manuscript and the very good comments, based on which we have prepared a revised manuscript. We first briefly describe general changes to manuscript, before going through the referees' comments individually and show how they have been addressed in the revision. Our answers to referee comments are set in boldface. The complete revised manuscript, highlighting the differences to the original version, is included at the end of this response letter. We hope the changes are deemed satisfactory and the revised manuscript will be accepted for publication.

Kind Regards,

Roope Halonen, Evgeni Zapadinsky, Theo Kurtén, Hanna Vehkamäki and Bernhard Reischl

1 General changes to the manuscript

- Based on the comments by referee 1, we have studied the temperature dependence of the collision rate coefficients and enhancement factors for the molecular dynamics simulation, the Langevin model, and the Brownian coagulation model. This is reflected in additions and changes in the results section, as well as:
 - new Appendix B: Temperature dependence of collision probabilities and interaction parameters
 - new Figure 7: Collision rate coefficient β (upper panel) and the enhancement factor W (lower panel) as a function of temperature calculated for the hard-sphere, MD, Langevin and Brownian approaches.
 - new Figure B1: Collision probabilities of sulfuric acid molecules, as a function of the impact parameter squared, for different values of the relative velocity, obtained from molecular dynamics simulation at 300 K (solid coloured lines), at 250 K (coloured dots) and at 400 K (coloured crosses). The step-like collision probabilities for a hard-sphere model ($b^2 = (2R)^2$), or obtained from the Langevin capture model, are indicated by the solid black, and dashed coloured lines, respectively.
 - new Table A1: The attractive potential parameters ϵ and r_0 for $\text{H}_2\text{SO}_4\text{-H}_2\text{SO}_4$ interaction based on the PMF calculations with the estimated anisotropic interaction factor $f = U_K/U$ and the corresponding enhancement factors calculated by the Langevin model W_L , anisotropic approach $W_{\text{aniso}}(f)$ and atomistic simulations W_{MD} .
- We have recalculated all numerical values reported in the manuscript. A few values have changed slightly as a consequence, but there are no quantitative changes to our results.
- The analytical expression for the collision rate enhancement factor over kinetic theory, using the Langevin model, has been simplified (Eq. 15).

2 Comments by Referee 1

This manuscript discusses calculation of the collision rate between two sulfuric acid molecules in the gas phase using molecular dynamics calculations. The authors find that the binding rate/collision rate is \sim a factor of 2.2 larger than would be expected based on hard sphere calculations. More detailed collision rate calculations are very important for molecules involved in new particle formation, as the resulting collision rate coefficients can be input into models of new particle formation and growth. This improves the accuracy and physical grounding of NPF models. I think this study is quite promising, very well-written, and the manuscript is easy to follow. However, I do think that calculation of the enhancement factor at a single temperature is of limited use; atmospheric systems are not all at a single temperature, and it is equally important to determine if the collision rate coefficient increases or decreases with temperature (i.e. its derivative). Fortunately, this should be possible to address in revision, and there are similar recent works (in very different systems) the authors could follow to address this issue, as noted below.

We thank referee 1 for the favorable assessment of our manuscript. The temperature dependence study has been carried out and is included in the revised manuscript.

Answers to Specific Comments:

1. Section 2.3. and Figure 5. The methods the authors use for binding rate coefficient calculations are nearly identical to those recently used by Yang, Goudeli, and Hogan (2018). Condensation and dissociation rates for gas phase metal clusters from molecular dynamics trajectory calculations. The Journal of Chemical Physics. 164304. It would be good to acknowledge that this approach has been utilized previously. In addition, in presenting results, Yang et al (2018) show collision probability contour plots as a function of (b,v) . I find these more intuitive to follow than Figure 5, thus I would recommend the authors look into providing these results as a contour plot.

We thank the referee for bringing this very relevant paper to our attention—we have now acknowledged it both in the introduction (“Recently, Yang et al. (2018) have studied the condensation rate coefficients for Au and Mg clusters at various gas temperatures using molecular dynamics calculations.”) and in the methods section (“The simulation setup is very similar to the one recently used by Yang et al. (2018).”).

We have also prepared a 2D density map of collision probability as a function of impact parameter and relative velocity in a similar style as in the reference mentioned above (see new Fig. 5). This replaces the original plot showing individual collision probabilities as function of impact parameter at a certain relative velocity in the results section. The original plot, including the new data obtained at 250 and 400 K has been moved to the new Appendix B, Fig. B1.:

“The statistics of the collision probabilities as a function of the impact parameter and relative velocity, $P(b,v)$, obtained from the atomistic simulations are shown as a heat map in Fig. 5 where white indicates a certain collision event (defined by the formation of one or more hydrogen bonds) and black indicates zero collision probability. [...] A more detailed plot is provided in Fig. B1, where the sigmoidal probability curves are shown for each velocity separately.”

2. Section 2.5. The collision between two un-ionized molecules in the gas phase at atmospheric pressure conditions is absolutely a free molecular process, and there is really no reason to compare the enhancement factor to the collision rate enhancement factor that applies in the continuum (diffusive or Brownian) limit. I would recommend removing it or altering the discussion to note that this calculation is simply included for reference, as it is not grounded in the correct transport physics for gas phase, molecular scale collisions. How the enhancement factor changes from the free molecular (ballistic) to transition to continuum (diffusive) regimes is discussed in Ouyang, Gopalakrishnan, and Hogan. (2012) Nanoparticle collisions in the gas phase in the presence of singular contact potentials. The Journal of Chemical Physics. 064316.

We agree with the referee – we mainly included this section because the Brownian coagulation model was used in the papers emphasising the discrepancy between experimental data and kinetic modelling of new particle formation (Kürten et al. (2014) and Lehtipalo et al. (2016)), but it was not explained in detail there. To clarify this, we have added the following “disclaimer” to the end of the section: “It should be noted that the model of Brownian coagulation does not describe the correct transport physics of collisions of molecules in the gas phase. For a discussion on the transition from the free molecular (ballistic) regime to the continuum (diffusive) regime, see e.g. Ouyang et al. (2012).”

3. Results and Discussion. I think a key issue to address in the manuscript is that presently the enhancement factor is only calculated at a single temperature. The evolution of it with temperature is of equal interest. Again, following Yang et al (2018) (Figures 5 and 6 of their work, in particular), I think this can be addressed to lead to an improved manuscript. First, using equation (10) of the current manuscript, the authors can vary the “translational” Temperature by shifting the Maxwell-Boltzmann distribution to see how the enhancement factor changes. Presumably, the enhancement factor decreases with increasing translational temperature, but it is not clear whether the actual collision rate coefficient increases or decreases with increasing temperature (in the hard sphere model it does, but many gas phase reactions have decreasing rates with increasing temperature). Of course, this approach neglects the changes in internal energies of the molecules, and adjusting internal energies the more time consuming effort of rerunning simulations with different initial equilibration

temperatures. Still, I would encourage the authors to do these calculations using at least one more temperature, to see how different they are from the results of simply shifting the equation (10) Maxwell-Boltzmann distribution. An enhancement factor calculated at a single temperature is of limited use if the temperature sensitivity is not explored and discussed.

We thank the referee for pointing out this limitation in our simulations and analyses – we have carried out a study of the temperature dependence of the collision rate coefficients as well as the enhancement factors over kinetic theory in a range of atmospherically relevant temperatures. Including the new results has led to many small additions and changes to the original manuscript. In the following, we summarize our additional study and the most important changes to the paper. For the full list of changes, we kindly refer to the manuscript with highlighted changes at the end of this response letter.

As the referee pointed out, temperature has a double effect on systems of colliding molecules: first, the Maxwell-Boltzmann distributions of relative velocities are different, and second, the rotational and vibrational motion of the molecules are different. In the calculation of collision coefficients from both the MD simulations as well as simpler models such as the Langevin approach, the first point can be addressed by carrying out the integration over the appropriate velocity distribution. However, the second point requires carrying out MD simulations at different temperature. In order to check the effect of temperature on the collision probabilities, we have rerun MD simulations with a subset of impact parameters with initial rotational and vibrational energies corresponding to 250 K and 400 K, as typical atmospheric processes will happen in this temperature range. These additional simulations indicate however that the differences in collision statistics at 250 K, 300 K, and 400 K, at a given relative velocity, are very small (see new Fig. B1). We therefore used the collision probability distributions calculated at $T = 300$ K, obtained for more values of b , to compute the collision rate coefficients and enhancement factors for the temperature range $T = 250$ –400 K. In this range, the collision rate coefficient is found to increase slightly with increasing temperature. The increase is smaller than in kinetic theory, where $\beta \sim T^{1/2}$ (see upper panel in new Fig. 7).

The Langevin model also has an explicit temperature dependence in the Maxwell-Boltzmann distribution, as well as a temperature dependence of the intermolecular interaction parameter ϵ . To address this we have carried out additional PMF calculations for the H_2SO_4 pair at $T = 250$ and 400 K. The collision rate coefficient obtained from the Langevin model in this temperature range is found to decrease with increasing temperature (see upper panel in Fig. 3). This is due to the neglect of the anisotropy of the dipole-dipole interactions in the Langevin model: at higher temperatures, the effect of anisotropy becomes less important and therefore the model overestimates the collision rate less, compared to lower temperatures.

In the temperature range 250-400 K, the collision enhancement compared to kinetic theory decreases with temperature both for the MD simulations, and the Langevin model. At higher temperatures, the enhancement factor obtained from the Langevin model approaches the MD value, for reasons discussed above (see lower panel in new Fig. 7). As we are interested in atmospheric new particle formation, we are not interested in temperatures outside of this range in the present work. We have added this discussion to the manuscript in the results and discussion, and simulation details have been added to a new section B in the appendix.

We have added the following paragraph in the results section:

“While the thermal velocity distribution $f(v)$ of the colliding molecules can be altered freely to correspond with an arbitrary temperature, the effect of the internal motion to the collision probability function is not necessarily temperature-invariant. However, in Appendix B it has been shown that a moderate change (simulations carried out at 250 and 400 K) in the internal kinetic energy does not affect the collision probabilities significantly. We therefore used the collision probability distributions calculated at 300 K to compute the collision rate coefficients for the atmospherically relevant temperature range $T=225$ -425 K (see Fig. 7).”

We have added the following paragraph in the conclusions:

“In the temperature range from 250 to 400 K, the rate enhancement factor is monotonously decreasing with increasing temperature, however the drop is less than 20 %. The velocity dependence of the simulated dynamical collision cross section is in good agreement with the Langevin model solution. We also note that the enhancement factor obtained from the Langevin

model using the attractive part of the intermolecular potential is a bit overestimated due to the imperfect treatment of the dipole-dipole interaction, yet in the atmospherically relevant temperature range the factor is within 30 % of the result from the atomistic simulation, at a fraction of the computational cost.”

4. Conclusions: After addressing comment 3 it is important to determine if the Langevin model is accurate at all temperatures, or just within 20% of calculations near 300 K. In addition, I think it would be good to discuss the implications of calculations for new particle formation and growth models more explicitly.

Regarding the accuracy of the Langevin model, we have added the following statement to the conclusions:

“[...] in the atmospherically relevant temperature range the [Langevin model enhancement] factor is within 30 % of the result from the atomistic simulation, at a fraction of the computational cost.”

Regarding the very last comment on the effect of collision rate enhancement on new particle formation rates, we note that in cluster dynamics codes such as ACDC (McGrath et al., 2012) detailed balance is assumed, and therefore global changes to the collision rates obtained by application of an enhancement factor are compensated by the corresponding changes in evaporation rates. However, in complex systems, individually changing collision rates for reactions that are close to the kinetic limit can change the preferred pathway for cluster growth, leading to different cluster distributions and particle formation rates.

We have added the following paragraph to the conclusions:

“However, before we can quantitatively assess the influence of collision rate enhancement on atmospherical new particle formation rates obtained from cluster dynamics models (for example ACDC (McGrath et al., 2012)), it is necessary to obtain the enhancement factors for all the relevant collisions between clusters of different sizes and composition, as the pathway for growth may change – a formidable task, even if only the simplest acid-base clusters were considered. Future work therefore should also be aimed at finding simple models for predicting approximate rate enhancements, based on just a few physico-chemical properties, such as molecular structures, dipole moments or charge distributions, of the interacting molecules and/or clusters.”

3 Comments by Referee 2

The authors calculate the collision rate of two sulfuric acid (SA) molecules in gas phase using atomistic molecular dynamics (MD) instead of the traditional hard sphere kinetic gas theory that is based on the diameter of sulfuric acid derived from its bulk liquid density. They benchmark two force fields for SA against ab initio results and conclude that an OPLS all-atom force field is better suited for the MD simulations. They find that the traditional kinetic gas theory underestimates the collision coefficient of two SA molecules by a factor of 2.2 compared to the MD simulations at 300 K. This discrepancy is consistent with empirical scaling used to match experimental new particle formation (NPF) rates and with those from theoretical ones employing hard sphere kinetics. They also explore other simpler models for calculating collision coefficients such as Brownian coagulation and Langevin dynamics. They find that both simpler models perform better than hard sphere kinetics and that their accuracy depends on the velocity of the colliding sulfuric acid molecules.

The work is promising in that it charts a new way to incorporate accurate collision rates into NPF rate calculations. The collision rate corrections for other species involved in sulfate aerosol formation are presumably larger than those for sulfuric acid, making this work particularly important. However, the authors need to address one critical point before the manuscript’s acceptance for publication. They have previously employed their Atmospheric Cluster Dynamics Code (ACDC) to calculate NPF rates for various sulfate aerosol systems. [McGrath, M. J., Olenius, T., Ortega, I. K., Loukonen, V., Paasonen, P., Kurtén, T., Kulmala, M., and Vehkamäi, H.: Atmospheric Cluster Dynamics Code: a Flexible Method for Solution of the Birth–Death Equations, *Atmos. Chem. Phys.*, 12, 2345–2355, <https://doi.org/10.5194/acp-12-2345-2012>, <http://www.atmos-chem-phys.net/12/2345/2012/>, 2012.] ACDC uses collision rates from hard sphere kinetics and evaporation rates from quantum mechanically derived Gibbs free energies to calculate the population of clusters and NPF rates. It would be appropriate for the authors to demonstrate how the cluster populations and NPF would change using collision rates from atomistic MD simulations. Such a comparison will also put the current work in the greater context of calculating NPFs which is the ultimate goal of studies like the current one.

We thank referee 2 for the favourable review of our manuscript. Regarding the general comment on the effect of collision rate enhancement on new particle formation rates, we note that in cluster dynamics codes such as ACDC (McGrath et al., 2012) detailed balance is assumed, and therefore global changes to the collision rates obtained by application of an enhancement factor are compensated by the corresponding changes in evaporation rates. However, in complex systems, individually changing collision rates for reactions that are close to the kinetic limit can change the preferred pathway for cluster growth, leading to different cluster distributions and particle formation rates.

We have added the following paragraph to the conclusions:

“However, before we can quantitatively assess the influence of collision rate enhancement on atmospheric new particle formation rates obtained from cluster dynamics models (for example ACDC, McGrath et al., 2012), it is necessary to obtain the enhancement factors for all the relevant collisions between clusters of different sizes and composition, as the pathway for growth may change—a formidable task, even if only the simplest acid-base clusters were considered. Future work therefore should also be aimed at finding simple models for predicting approximate rate enhancements, based on just a few physico-chemical properties, such as molecular structures, dipole moments or charge distributions, of the interacting molecules and/or clusters.”

Answers to Specific Comments:

1. Page 1, line 19: Define “impact parameter”

We have added the following clarification in the introduction: “[...] the impact parameter i.e. the perpendicular distance between the spheres’ trajectories [...]”

2. Page 2, line 8-10: The following statement is important enough to warrant a more detailed discussion. “In fact, it has recently been found that collision coefficients obtained in this way had to be scaled by a factor 2.3–2.7 to predict kinetically limited nucleation rates in agreement with experiment, for a system containing sulfuric acid, dimethylamine and water (Kürten et al., 2014; Lehtipalo et al., 2016; Kürten et al., 2018).”

We have made the following change to the sentence in the manuscript: “In fact, systematic discrepancies have been found between experimental particle formation rates and values predicted from kinetic modelling and cluster dynamics simulations, where hard-sphere collisions are assumed. Kürten et al. (2014) measured the kinetic formation rate of sulphuric acid dimers and found that an enhancement factor of 2.3 needed to be applied to the formation rate obtained from a kinetic model. Lehtipalo et al. (2016) and Kürten et al. (2018) have studied particle formation rates in systems containing sulphuric acid, dimethylamine and water and concluded that an enhancement factor of 2.7 and 2.3, respectively, was needed to match experimental particle formation rates.”

3. Page 2, line 11: Define “capture rate constant” and how it differs from “collision rate constant”. If collision and capture rates are the same for the purposes of this work, the authors should stick with one or the other for the sake of clarity.

We apologize for the lack of clarity regarding the difference between collision and capture. We have added the following paragraph to section 2.4: “As the collision rate in the context of atomistic simulations is defined as the reaction rate of hydrogen bonding, the related theoretical models are often based on the assumption that if the trajectory of the colliding molecules is able to surmount a centrifugal barrier the reaction is certain. This is known as the capture approximation; to emphasise this conceptual difference between simulations and theoretical models, we use the word *capture* instead of *collision* to refer to theory-based results.”

4. Page 3, Section 2.1: What are the exact forms of the Ding and Loukonen/OPLS force fields? What terms are included? Which one is more flexible? Including this information will be instructive to the reader.

We have added the following description of the functional forms of the inter- and intramolecular potentials to the methods section:

“In both force fields intermolecular interactions are described by the sum of Lennard-Jones potentials between atoms i and j separated by a distance r_{ij} , with distance and energy parameters

σ_{ij} and ε_{ij} , and Coulomb interactions between the partial charges q_i and q_j ,

$$U_{\text{inter}} = \sum_{i=1}^{N_1} \sum_{j=1}^{N_2} 4\varepsilon_{ij} \left[\left(\frac{\sigma_{ij}}{r_{ij}} \right)^{12} - \left(\frac{\sigma_{ij}}{r_{ij}} \right)^6 \right] + \sum_{i=1}^{N_1} \sum_{j=1}^{N_2} \frac{1}{4\pi\epsilon_0} \frac{q_i q_j}{r_{ij}}. \quad (1)$$

However, in the force field by Ding et al., the geometry of the individual molecule is simply constrained by harmonic potentials with force constants k_{ij} between all pairs of atoms,

$$U_{\text{intra}}^{\text{Ding}} = \sum_{i=1}^{N_1-1} \sum_{j=i+1}^{N_1} \frac{k_{ij}}{2} (r_{ij} - r_{ij}^0)^2, \quad (2)$$

while in OPLS the intramolecular interactions consist of the usual sum of two, three, and four-body potentials, i.e. harmonic bonds between covalently bonded atoms, harmonic angles θ between atoms separated by two covalent bonds, and torsions (dihedral angles ϕ) between atoms separated by three covalent bonds,

$$U_{\text{intra}}^{\text{OPLS}} = \sum_{i=1}^{N_{\text{bonds}}} \frac{k_i^b}{2} (r_i - r_i^0)^2 + \sum_{j=1}^{N_{\text{angles}}} \frac{k_j^\theta}{2} (\theta_j - \theta_j^0)^2 + \sum_{k=1}^{N_{\text{dihedrals}}} \sum_{n=1}^4 \frac{V_n}{2} [1 + \cos(n\phi^k - \phi_n^k)]. \quad (3)$$

5. Page 4, Figure 1: The authors should label the different hydrogen bonds in the figure to facilitate cross-referencing with the d[O...H] lines in Table 1.

We have numbered the hydrogen bonds for dimer structures a-d in Fig. 1 and added the corresponding hydrogen bond number to the hydrogen bond distance values in the Tab. 1.

6. Page 4, Table 1: It is curious that the authors benchmark the two force fields against a 2012 paper while more recent and more rigorous computational results should be available. The authors should reference other high quality works on the sulfuric acid dimer and justify their choice to use the 2012 paper as a benchmark.

The paper by Temelso et al. (2012) is to our knowledge the only reference that contains detailed information on potential/electronic energies and hydrogen bond geometries for different conformers of the H₂SO₄ dimer, as well as the binding free energy. For the binding free energies, we found reasonable agreement between the study by Temelso et al. (2012) and more recent work by Elm et al. (2016) and Myllys et al. (2017), which we do mention in the manuscript. Note that Temelso et al. have obtained the binding free energy from Boltzmann-averaging over the four minimum energy dimer structures, while in the newer references only the global minimum energy structure has been considered, this detail has also been added to the paragraph.

7. Page 4, Table 1: It is curious why the authors use eV units for their $\Delta\Delta E$ values while the most commonly used unit is kcal mol⁻¹.

In computational physics and chemistry, commonly used units of energy are eV, kJ/mol, kcal/mol, or $k_B T$. The unit used in the LAMMPS simulation in/output was eV, which is why this was the most natural choice for the manuscript. Since none of the important quantities we report, such as the collision rate coefficients, or enhancement factors, have the unit of energy, we think this should not be a major concern. However, to accomodate all audiences, we have added the conversion factors at the bottom of Table 1: “Energy unit conversion: 1 eV \approx 96.49 kJ·mol⁻¹ \approx 23.06 kcal·mol⁻¹ \approx 38.68 $k_B T$ at $T = 300$ K.”

8. Page 8, line 16: “diameters of 49-127nm” seems incorrect. Perhaps the units are wrong.

The values cited in our manuscript indeed correspond to the values given in the paper by Chan and Mozurkewich (2001), both in the abstract and in Fig. 5.

Rate enhancement in collisions of sulfuric acid molecules due to long-range intermolecular forces

Roope Halonen¹, Evgeni Zapadinsky¹, Theo Kurtén², Hanna Vehkamäki¹, and Bernhard Reischl¹

¹Institute for Atmospheric and Earth System Research / Physics, Faculty of Science, University of Helsinki, P.O. Box 64, FI-00014, Finland

²Institute for Atmospheric and Earth System Research / Chemistry, Faculty of Science, University of Helsinki, P.O. Box 55, FI-00014, Finland

Correspondence: Roope Halonen (roope.halonen@helsinki.fi)

Abstract. Collisions of molecules and clusters play a key role in determining the rate of atmospheric new particle formation and growth. Traditionally the statistics of these collisions are taken from kinetic gas theory assuming spherical non-interacting particles, which may significantly underestimate the collision coefficients for most atmospherically relevant molecules. Such systematic errors in predicted new particle formation rates will also affect large-scale climate models. We have studied the statistics of collisions of sulfuric acid molecules in vacuum by atomistic molecular dynamics simulations. We have found that the effective collision cross section of the H₂SO₄ molecule, as described by an OPLS-All Atom force field, is significantly larger than the hard-sphere diameter assigned to the molecule based on the liquid density of sulfuric acid. As a consequence, the actual collision coefficient is enhanced by a factor 2.2 [at 300 K](#), compared to kinetic gas theory. This enhancement factor obtained from atomistic simulation is consistent with the discrepancy observed between experimental formation rates of clusters containing sulfuric acid and calculated formation rates using hard sphere kinetics. We find reasonable agreement with an enhancement factor calculated from the Langevin model of capture, ~~fitted to~~ [based on](#) the attractive part of the atomistic intermolecular potential of mean force.

1 Introduction

New particle formation from condensable vapours gives an important contribution to the composition of aerosols in the atmosphere which affects air quality as well as the Earth's climate. The positive and negative contributions of atmospheric aerosols to the planet's radiative balance are still not fully understood, and currently constitute one of the largest uncertainties in climate modelling. The earliest stage of new particle formation involves collisions of individual molecules leading to the appearance of a new molecular complex. In many theoretical approaches, the statistics of such collisions are simply taken from kinetic gas theory, i.e. the molecules are considered to be non-interacting hard spheres, and a collision occurs when the impact parameter [i.e. the perpendicular distance between the spheres' trajectories](#) is smaller than the sum of the hard spheres' radii. The hard sphere collision cross section is independent of the relative velocity of the colliding bodies, and the collision rate coefficient

for hard spheres of identical radii is customarily expressed as

$$\beta_{\text{HS}} = \sqrt{\frac{8k_{\text{B}}T}{\pi\mu}}\pi(2R)^2, \quad (1)$$

where k_{B} is Boltzmann's constant, T is the temperature, μ is the reduced mass and R is the radius of the spheres.

25 It is well known that acid-base clusters, and in particular clusters containing sulfuric acid and ammonia, or amines, are very relevant in nucleation and growth of particles that can serve as cloud condensation nuclei (Almeida et al., 2013). Such molecules, however, are not necessarily spherical and despite being charge neutral, exhibit long-ranged attraction due to interactions between permanent dipoles, permanent and induced dipoles, or induced dipoles (Israelachvili, 2011). Therefore, it is reasonable to expect that particle growth rates or cluster size distributions predicted using collision coefficients from kinetic
30 gas theory will have a systematic error, which needs to be accounted for. In fact, ~~it has recently been found that collision coefficients obtained in this way had to be scaled by a factor~~ systematic discrepancies have been found between experimental particle formation rates and values predicted from kinetic modelling and cluster dynamics simulations, where hard-sphere collisions are assumed. Kürten et al. (2014) measured the kinetic formation rate of sulphuric acid dimers and found that an enhancement factor of 2.3 ~~-2.7 to predict kinetically limited nucleation rates in agreement with experiment, for a system~~
35 ~~containing sulfuric~~ needed to be applied to the formation rate obtained from a kinetic model. Lehtipalo et al. (2016) and Kürten et al. (2018) have studied particle formation rates in systems containing sulphuric acid, dimethylamine and water (Kürten et al., 2014; Lehtipalo et al., 2016; Kürten et al., 2018). ~~and concluded that an enhancement factor of 2.7 and 2.3, respectively, was needed to match experimental particle formation rates.~~

The effect of long-range interactions between neutral polar molecules on the capture rate constant has been studied by classical trajectory integration (Maergoiz et al., 1996c). The interaction potential between the colliding parties has been approximated by two terms: First, an anisotropic interaction between permanent dipoles, proportional to r^{-3} , where r is the distance between the centres of mass of the molecules. Second, an isotropic term due to the interaction between permanent dipole and induce dipole, and the interaction between induced dipoles, proportional to r^{-6} . However, such an approximation is inaccurate when the distance between the colliding particles is comparable to their size. Rate coefficients for ion-molecule capture processes
45 have also been studied theoretically in both classic and quantum regime (Moran and Hamill, 1963; Su and Bowers, 1973; Su et al., 1978; Chesnavich et al., 1980; Clary, 1985; Troe, 1987) or by using trajectory calculations (Dugan Jr. and Magee, 1967; Chesnavich et al., 1980; Su and Chesnavich, 1982; Maergoiz et al., 1996a, b). Atomistic simulations have been used to study collisions of Lennard-Jones clusters and atmospherically relevant molecules, but these studies did not analyze or report thermal collision rate coefficients (Napari et al., 2004; Loukonen et al., 2014). Recently, Yang et al. (2018) have studied the
50 condensation rate coefficients for Au and Mg clusters at various gas temperatures using molecular dynamics calculations. The influence of Van der Waals forces on the collision rate has also been considered in Brownian coagulation models of ultra-fine aerosol particles (Marlow, 1980; Sceats, 1986, 1989).

In the present work, we use atomistic molecular dynamics simulations to study the statistics of collisions between sulfuric acid molecules in vacuum, determine the collision rate coefficient and calculate the enhancement factor over kinetic gas theory.
55 We are here focusing on "reactive" collisions, defined by the formation of one or more hydrogen bonds between the molecules.

Detailed modelling of e.g. proton transfer processes related to hydrogen bond formation in such reactive collisions would require first principle simulations (Loukonen et al., 2014), however the need to simulate a large number of individual trajectories to cover a representative range of impact parameters and relative velocities makes this impossible. In the present study we are modelling the collision rate enhancement due to long-range interactions, which can be decently described by empirical force fields.

In section 2 we discuss technical matters of the choice of force field and the simulation setup and give a brief overview of the theoretical background for collisions of atmospheric particles. In section 3, simulation results are presented, discussed within the theoretical framework and compared to analytical and experimental results.

2 Simulation details and theoretical models

2.1 Force field benchmark

We have considered two force fields to describe the sulfuric acid molecules in the present study. The first choice was the force field by Ding et al. (2003), fitted specifically to reproduce DFT structures and energies of small clusters of sulfuric acid, bisulfate and water, in vacuum. The second choice was the force field by Loukonen et al. (2010), who had fitted interaction parameters for sulfuric acid, bisulfate and dimethylammonium according to the OPLS-All Atom procedure (Jorgensen et al., 1996). Both force fields are fitted to reproduce the C_2 geometry of the isolated H_2SO_4 molecule in vacuum, and the atoms' partial charges create dipole moments of 3.52 and 3.07 Debye, for Ding et al. and Loukonen et al., respectively, in agreement with experiments (2.7–3.0 Debye) and ab initio calculations (2.7–3.5 Debye) (Sedo et al., 2008). While in the OPLS force field intramolecular degrees of freedom are described by harmonic bonds and angles as well as dihedrals, the geometry of the molecule is simply constrained by harmonic potentials with force constants k_{ij} between all pairs of atoms.

$$\begin{aligned}
 U_{\text{inter}} &\approx \sum_{i=1}^{N_1} \sum_{j=1}^{N_2} 4\epsilon_{ij} \left[\left(\frac{\sigma_{ij}}{r_{ij}} \right)^{12} - \left(\frac{\sigma_{ij}}{r_{ij}} \right)^6 \right] \\
 &\quad + \sum_{i=1}^{N_1} \sum_{j=1}^{N_2} \frac{1}{4\pi\epsilon_0} \frac{q_i q_j}{r_{ij}}.
 \end{aligned} \tag{2}$$

However, in the force field by Ding et al. is constrained using additional intramolecular harmonic potentials between non-bonded atoms, the geometry of the individual molecule is simply constrained by harmonic potentials with force constants k_{ij} between all pairs of atoms.

$$U_{\text{intra}}^{\text{Ding}} = \sum_{i=1}^{N_1-1} \sum_{j=i+1}^{N_1} \frac{k_{ij}}{2} (r_{ij} - r_{ij}^0)^2, \tag{3}$$

while in OPLS the intramolecular interactions consist of the usual sum of two, three, and four-body potentials, i.e. harmonic bonds between covalently bonded atoms, harmonic angles θ between atoms separated by two covalent bonds, and torsions

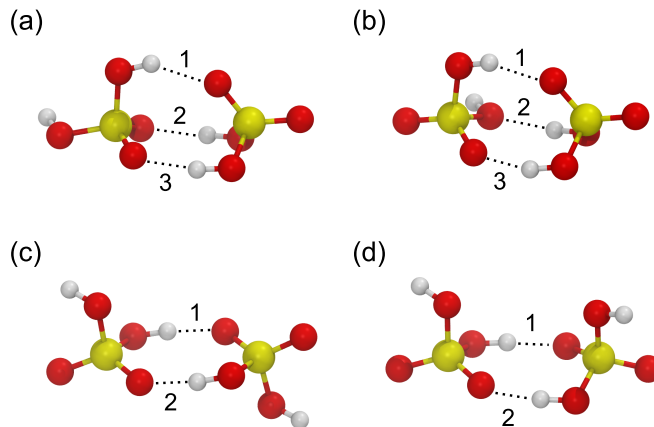


Figure 1. Four minimum energy structures for the sulfuric acid dimer (a–d) used to benchmark the force fields by Ding et al. (2003) and Loukonen et al. (2010) against ab initio calculations by Temelso et al. (2012). Sulfur atoms are yellow, oxygens red and hydrogens white. Hydrogen bonds are indicated by dotted lines [and enumerated according to Tab. 1.](#)

[\(dihedral angles \$\phi\$ \) between atoms separated by three covalent bonds,](#)

$$\begin{aligned}
 85 \quad U_{\text{intra}}^{\text{OPLS}} &\cong \underbrace{\sum_{i=1}^{N_{\text{bonds}}} \frac{k_i^b}{2} (r_i - r_i^0)^2}_{\text{bonds}} + \underbrace{\sum_{j=1}^{N_{\text{angles}}} \frac{k_j^\theta}{2} (\theta_j - \theta_j^0)^2}_{\text{angles}} \\
 &\pm \underbrace{\sum_{k=1}^{N_{\text{dihedrals}}} \sum_{n=1}^4 \frac{V_n}{2} [1 + \cos(n\phi^k - \phi_n^k)]}_{\text{dihedrals}}. \tag{4}
 \end{aligned}$$

To validate the force fields, we compare the structures and energies of four stable configurations of the sulfuric acid dimer illustrated in Fig. 1(a–d) to ab initio structures and energies at the RI-MP2/CBS//6-31+G* level of theory calculated by Temelso et al. (2012). The results of the benchmark are summarised in Tab. 1. The force field by Ding et al. correctly predicts the lowest energy for dimer structure “a”, and the relative energy differences $\Delta\Delta E$ between optimised structures are closer to those obtained in the ab initio calculation than for the OPLS force field, which assigns the lowest energy to structure “d”, which is the highest energy structure in the ab initio calculation. The geometries of the structures agree well with the ab initio result for both force fields, with the OPLS force field reproducing the ab initio hydrogen bond lengths slightly better than the force field by Ding et al. The binding energies at $T = 0$ K are slightly lower for the force fields (–0.64 and –0.67 eV for OPLS, and Ding et al., respectively) compared to the ab initio value of –0.72 eV. Overall, the force field by Ding et al. performs slightly better in terms of energetics.

However, the vibrational spectra, calculated from the Fourier transform of the velocity autocorrelation functions of an isolated H_2SO_4 molecule in vacuum, exhibit strong differences: while the force field by Loukonen et al. is able to reproduce the experimental and ab initio spectra very well (Hintze et al., 2003; Chackalackal and Stafford, 1966; Miller et al., 2005), the force field by Ding et al. is not, as shown in Fig. 2. Intramolecular vibrations are relevant in the context of molecular colli-

sions, e.g. when studying energy transfer between different internal degrees of freedom during, and after the collision. Also, the OPLS-All Atom procedure allows for transferable potentials, as opposed to the Ding et al. force field which cannot easily be extended to other chemical compounds in future studies. For these two reasons, we decided to use the OPLS force field by Loukonen et al. for the collision simulations.

105 2.2 Potential of mean force of two sulfuric acid molecules

We first calculated the binding free energy of two sulfuric acid molecules in vacuum as described by the force fields of Loukonen et al. and Ding et al. The potential of mean force (PMF) as a function of the sulfur–sulfur distance was calculated from a well-tempered metadynamics simulation (Barducci et al., 2008), using the PLUMED plug-in (Tribello et al., 2014) for LAMMPS (Plimpton, 1995). We used a Velocity Verlet integrator with a time step of 1 fs, to correctly resolve the motion of
 110 the hydrogen atoms. The Lennard-Jones interactions were cut off at 14 Å and electrostatic interactions were only evaluated in direct space, with a cut-off at 40 Å. We employed 24 random walkers and Gaussians with a width of 0.1 Å and initial height of $k_B T$ were deposited every 500 steps along the collective variable and a harmonic wall was used to restrict it to values below 35 Å. A bias factor of 5 was chosen, and a Nosé–Hoover chain thermostat of length 5 with a time constant of 0.1 ps was used to keep a temperature $T = 300$ K. The combined length of the trajectories was 120 ns for each force field. Both PMFs, shown

Table 1. Relative energies $\Delta\Delta E$ (eV) and hydrogen bond distances $d_{O\dots H}$ (Å) for the sulfuric acid dimer structures (a–d) in Fig. 1 obtained from [ab initio calculations by Temelso et al. \(2012\)](#) and with the force fields by Ding et al. (2003) and Loukonen et al. (2010) ~~and from ab initio calculations by Temelso et al. (2012), following the OPLS doctrine.~~

Structure		a	b	c	d	
$\Delta\Delta E$ (eV)	Temelso et al. ab initio	0.000	0.032	0.036	0.048	
	Ding et al.	0.000	0.081	0.052	0.045	
	Loukonen et al. OPLS	0.180	0.099	0.004	0.000	
$d_{O\dots H}$ (Å)	Temelso et al. ab initio	1	<u>1.82</u>	1.74	1.75	1.75
		<u>2</u>	1.89	1.91	1.75	1.75
		<u>3</u>	1.90	1.87		
	Ding et al.	<u>1</u>	2.00	1.84	1.75	1.74
		<u>2</u>	1.87	2.31	1.74	1.74
		<u>3</u>	1.88	1.85		
	Loukonen et al. OPLS	<u>1</u>	1.91	1.84	1.72	1.72
		<u>2</u>	1.85	1.87	1.72	1.72
		<u>3</u>	1.83	1.83		

Energy unit conversion: 1 eV \approx 96.49 kJ·mol⁻¹ \approx 23.06 kcal·mol⁻¹ \approx 38.68 $k_B T$ at $T = 300$ K.

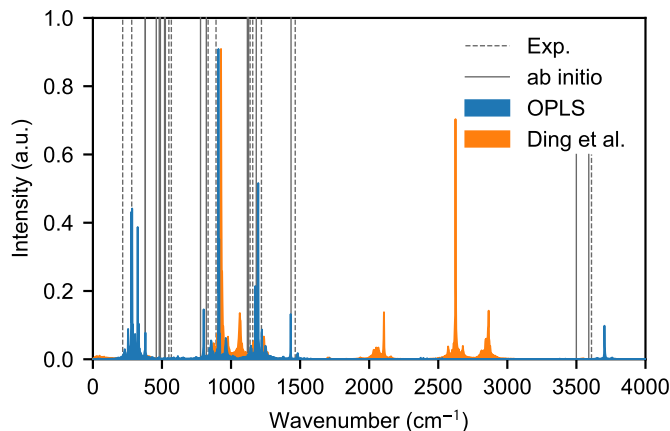


Figure 2. Vibrational spectra of the sulfuric acid molecule obtained with OPLS (Loukonen et al., 2010) (blue area) and the force field by Ding et al. (2003) (orange area). The spectra of Ding et al. has its highest frequency mode at 6565 cm^{-1} outside of the range of the figure. The positions of the peaks in the experimental spectra (Hintze et al., 2003; Chackalackal and Stafford, 1966; Miller et al., 2005) and ab initio calculations (Miller et al., 2005) are indicated by dashed and solid grey lines, respectively.

115 in Fig. 3, exhibit a minimum at $r = 4.1\text{ \AA}$, and the binding free energies are $\Delta F = -0.29\text{ eV}$ and -0.27 eV for Loukonen et al., and Ding et al., respectively. This is in excellent agreement with the ab initio value of $\Delta G = -0.30\text{ eV}$ obtained from ab initio calculations Boltzmann-averaging over the four minimum energy dimer structures by Temelso et al. (2012) at 298.15 K , and more recent calculations at higher level of theory, which predict slightly weaker binding (-0.23 to -0.26 eV) (Elm et al., 2016; Myllys et al., 2017).

120 2.3 Collision simulation setup

Molecular dynamics simulations were performed with the LAMMPS code, using a Velocity Verlet integrator with a time step of 1 fs . The Lennard-Jones interactions were cut off at 14 \AA and electrostatic interactions were only evaluated in direct space, with a cut-off at 120 \AA . The simulations were carried out in the NVE ensemble, as the colliding molecules constitute a closed system (in atmospheric conditions collisions with the carrier gas are rare on the time scale of collisions between sulfuric acid molecules). In order to determine the molecules' collision probability as a function of impact parameter and relative velocity, the following setup was used: first, two sulfuric acid molecules were placed in the simulation box, separated by 100 \AA along x and the impact parameter b was set along the z direction, ranging from 0 to 17.5 \AA in steps of 0.5 \AA . Atomic velocities were randomly assigned from a Maxwell-Boltzmann distribution at $T = 300\text{ K}$, and the centre of mass motion of each molecule removed separately. Then the system was evolved for 50 ps , to randomise the intermolecular orientation and ensure equipartition of energy along the intramolecular degrees of freedom. At $t = 50\text{ ps}$, each molecule received a translational velocity along the x direction, $v_x = \pm v/2$, where v denotes the relative velocity, to set them on a potential collision course. The simulation was continued for another 250 ps , to ensure the possibility of a collision, even at the smallest relative velocities.

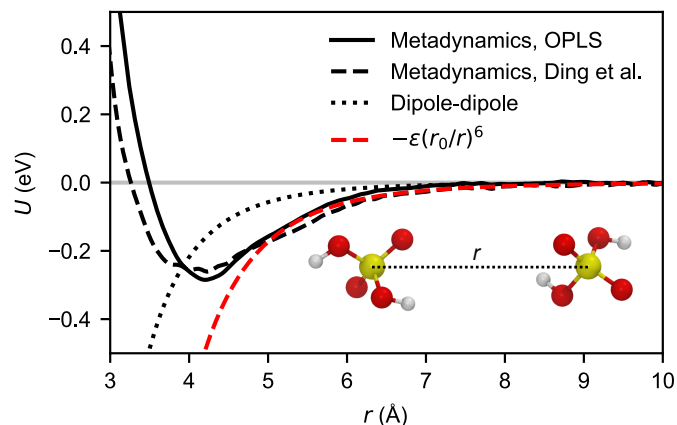


Figure 3. Potential of mean force between two H_2SO_4 molecules as a function of the sulfur–sulfur distance calculated by metadynamics simulation for the OPLS force field (Loukonen et al., 2010) (solid black line) and the force field by Ding et al. (2003) (dashed black line) at 300 K. For comparison, the Keesom (thermally averaged permanent dipole–permanent dipole) interaction between two point dipoles (see Eq. (A11)) of 3.07 Debye at 300 K is depicted by the dotted line. The dashed red line shows the attractive potential (Eq. (8)) fitted to based on the tail of the calculated PMF curve of the OPLS force field.

For a collision of two identical molecules with molecular mass m , the relative velocities follow the Maxwell–Boltzmann distribution with reduced mass $\mu = m/2$. We sampled relative velocities between 50 and 800 ms^{-1} , in steps of 50 ms^{-1} . 99 % of the distribution lies within this range at $T = 300$ K. For each value of the impact parameter b and the relative velocity v , 1000 simulations were carried out starting with different initial atomistic velocities, to ensure good sampling. The simulation setup is very similar to the one recently used by Yang et al. (2018). Sulfuric acid molecules bind to each other through the formation of one or more hydrogen bonds. However, even if a collision course leads to an attachment of the two molecules, a portion of the kinetic energy will be redistributed on the degrees of freedom of the formed complex, and this excess energy can lead to a rapid dissociation in the absence of a thermalizing medium. To automate the analysis of over half a million individual trajectories, we define a collision as a trajectory during which the electrostatic energy (E_{Coul}) is lower than a threshold value of -0.25 eV in at least 10 consequent frames (100 psfs), indicative of the formation of one or more hydrogen bonds. Three examples of simulated trajectories with relative velocity closest to the mean velocity at 300 K (350 ms^{-1}) and impact parameter of 8.5 Å are illustrated in Fig. 4.

The results from the atomistic simulations will be compared to different theoretical models described in the following.

2.4 Classical model of capture in a field of force

As the collision rate in the context of atomistic simulations is defined as the reaction rate of hydrogen bonding, the related theoretical models are often based on the assumption that if the trajectory of the colliding molecules is able to surmount a

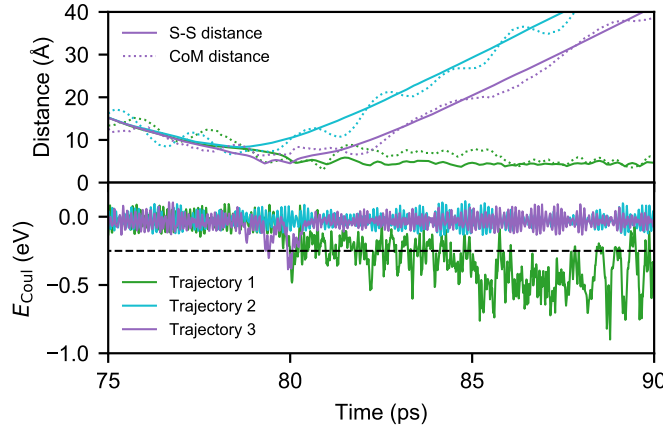


Figure 4. Three example MD trajectories with relative velocity of 350 ms^{-1} and impact parameter of 8.5 \AA after 50 ps of energy relaxation and first 25 ps of collision simulation. The upper panel shows both the distance between the two sulfur atoms (solid lines) and the centre-of-mass distance of the molecules (dotted lines) during the simulations. The electrostatic energies E_{Coul} , which is used to determine the possible collision event, for successful (1), unsuccessful (2) and successful but instantly evaporating (3, continuously 0.18 ps below the threshold) trajectories are shown in the lower panel with the threshold value (dashed black line).

150 centrifugal barrier the reaction is certain. This is known as the capture approximation; to emphasise this conceptual difference between simulations and theoretical models, we use the word *capture* instead of *collision* to refer to theory-based results.

The interaction between two identical polar molecules is usually written as

$$V = \frac{(\mathbf{d}_1 \cdot \mathbf{d}_2) - 3(\mathbf{d}_1 \cdot \mathbf{n})(\mathbf{d}_2 \cdot \mathbf{n})}{r^3} + U(r), \quad (5)$$

155 where \mathbf{d}_1 and \mathbf{d}_2 are the dipole moment vectors of the molecules, \mathbf{n} is the unit vector along the distance vector \mathbf{r} connecting the centres of mass of the molecules, and $U(r)$ is a spherically symmetric potential, usually proportional to r^{-6} . The capture rate constant for such a potential can only be calculated numerically (Maergoiz et al., 1996c). In the present section we consider only the isotropic part $U(r)$ of the interaction described by Eq. (5), the effect of anisotropic part (first term in Eq. (5)) is discussed in Appendix A. Then, the Langevin model of capture (Langevin, 1905) can be used to calculate the critical impact parameter beyond which point-like colliding particles in vacuum will escape from each other. Here, the motion of the two colliding molecules is reduced to a one-body problem in an external central field by using an effective potential containing
160 dispersion and centrifugal terms (Landau and Lifshitz, 1976),

$$U_{\text{eff}}(r) = U(r) + \frac{L^2}{2\mu r^2}, \quad (6)$$

where r is the distance of the colliding body from the centre of the field, L the angular momentum. Both the total energy of the system (which equals the initial translational energy $\mu v^2/2$ at $r \rightarrow \infty$) and the angular momentum are conserved. The centrifugal term introduces an energy barrier, and for a successful capture at the barrier ($r = r_{\text{max}}$) the translational energy

165 $\mu \dot{r}_{\max}^2/2$ has to be positive. Since the angular momentum equals $L = \mu v b$, the condition for b^2 to ensure a capture is

$$b^2 < r_{\max}^2 \left(1 - \frac{2U(r_{\max})}{\mu v^2} \right). \quad (7)$$

In case of a simple attractive potential (repulsive forces can be neglected, as the studied velocities are relatively low),

$$U(r) = -\epsilon \left(\frac{r_0}{r} \right)^6, \quad (8)$$

the square of the critical impact parameter can be written as

$$170 \quad b_c^2 = \left(\frac{27\epsilon}{2\mu v^2} \right)^{1/3} r_0^2. \quad (9)$$

It is preferable to consider the squared value of b , since the capture cross section is calculated as $\sigma_c = \pi b_c^2$. It is important to note that in the Langevin model, the total energy is divided strictly to the translational and potential energy, the internal degrees of freedom of the two bodies are considered to be completely decoupled, i.e. exchange of translational energy to rotations and vibrations that will occur in a real molecule is completely neglected.

175 ~~To compare the Langevin model to atomistic simulation results using the OPLS force field, we fitted a potential described by Eq. (8) to the attractive part of the PMF from metadynamics, shown in Fig. 3, and obtained the parameters $\epsilon = 0.57$ eV and $r_0 = 4.1$ Å.~~

2.5 Brownian model of aerosol coagulation

In the study by Kürten et al. (2014), a model of Brownian coagulation in a field of force (Sceats, 1986, 1989) was used to
 180 estimate the collision enhancement factor for neutral cluster formation involving sulfuric acid in a free molecule regime (Chan and Mozurkewich, 2001). The model is based on solving the Fokker–Planck equation for a pair of Brownian particles whose motion is determined by a thermal random force (Sceats, 1986). In the paper by Chan and Mozurkewich (2001), the Hamaker constant describing the strength of the van der Waals interaction was fitted to experiments with uncharged H₂SO₄/H₂O particles with diameters of 49–127 nm, yielding a collisions enhancement factor value of 2.3 at 300 K. Although the Hamaker constant
 185 is usually considered to be size-independent, there may be enhanced interaction for very small particle sizes, with radii of the order of 1 nm (Pinchuk, 2012).

For the attractive potential described by Eq. (8), the collision enhancement factor over the kinetic gas theory rate, $W_B = \beta_B/\beta_{HS}$, from the Brownian coagulation model in the free molecule limit can be written as (Sceats, 1989)

$$W_B = \left(\frac{3\epsilon}{k_B T} \right)^{1/3} \left(\frac{r_0}{2R} \right)^2 \exp\left(\frac{1}{3} \right); \quad (10)$$

190 ~~where ϵ and r_0 are the fitted potential parameters to be equal to $-2\Delta F$ and the sulfur-sulfur distance at which the PMF reaches its minimum, respectively.~~

It should be noted that the model of Brownian coagulation does not describe the correct transport physics of collisions of molecules in the gas phase. For a discussion on the transition from the free molecular (ballistic) regime to the continuum (diffusive) regime, see e.g. Ouyang et al. (2012).

195

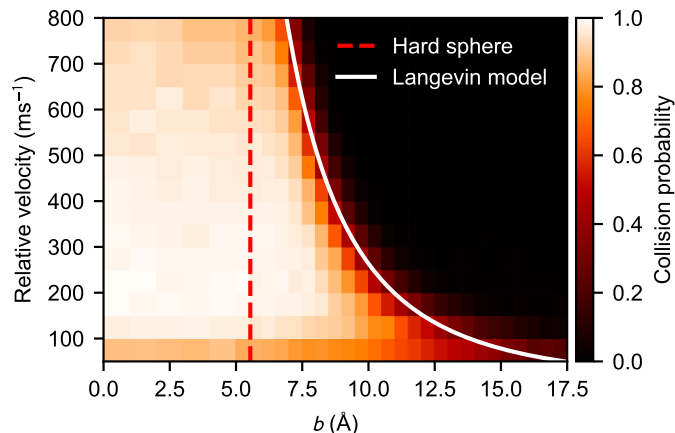


Figure 5. Collision probabilities Heat map of the collision probability of sulfuric acid molecules, plotted as a function of the impact parameter squared, for different values of the b and relative velocity v obtained from molecular dynamics simulation (solid coloured lines). The step-like collision probabilities for a impact parameter equivalent to the hard-sphere model collision area ($b^2 = (2R)^2$ $b = 2R$), or and the critical impact parameter obtained from the Langevin capture model (Eq. (9)), are indicated by the solid black, and dashed coloured red and the solid white lines, respectively.

3 Results and Discussion

The statistics of the collision probabilities as a function of the square of the impact parameter impact parameter and relative velocity, $P(b, v)$, $P(b^2)$, obtained from the atomistic simulations are shown as a heat map in Fig. 5. The shapes of the simulated curves are sigmoidal and where white indicates a certain collision event (defined by the formation of one or more hydrogen bonds) and black indicates zero collision probability. The critical impact parameter (above which a collision unlikely occurs) has a negative exponential dependency on the relative velocity, which corresponds well with the Langevin model. A more detailed plot is provided in Fig. B1, where the sigmoidal probability curves are shown for each velocity separately. Predominantly, the collision probability is close to unity as b approaches zero approaches to unity with lower relative velocity and shorter impact parameter. However, the collision probability decreases slightly at high relative velocities where rapid re-

200
205

210 The dynamical collision cross section, obtained from the integral over the collision probability functions,

$$\sigma_d(v) = \pi \int_0^{\infty} db^2 P(b^2, v), \quad (11)$$

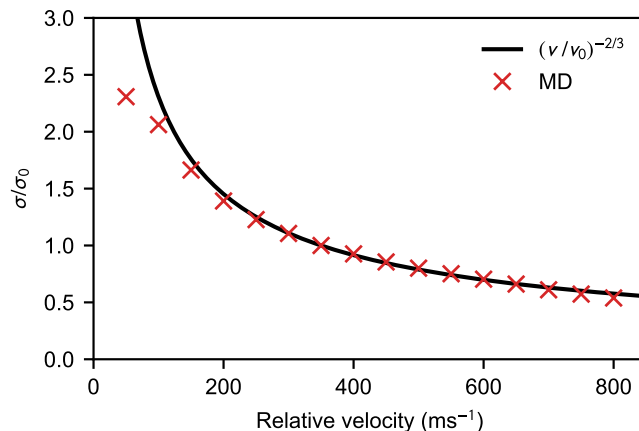


Figure 6. Ratio between collision cross section σ and a reference value σ_0 as a function of relative velocity. Here the reference value σ_0 is the cross section corresponding to relative velocity $v_0 = 350 \text{ ms}^{-1}$. The red crosses show the ratio of dynamical cross sections obtained from MD simulations, and the solid black line shows the relation predicted by the Langevin model in Eq. (12).

is consistently decreasing with relative velocity v . Even though it can be clearly seen in Fig. 5, and especially in Fig. B1, that values of σ_d are smaller than the corresponding Langevin capture cross sections σ_c , the velocity dependence of the change in σ_d is in very close agreement with the Langevin model solution

$$215 \quad \frac{\sigma_c(v)}{\sigma_c(v_0)} = \left(\frac{v}{v_0} \right)^{-2/3}, \quad (12)$$

where v_0 is a reference velocity, as shown in Fig. 6. The importance of contributions from long-ranged interactions to the collision cross section is evident, as σ_c is proportional to $v^{-4/n}$, for interactions decaying with r^{-n} . Furthermore, as can be seen in Fig. 5B1, the critical impact parameters from the Langevin model are matching rather well with the tails of the simulated collision probability curves, the intersection is located without exception at $P(b^2) \approx 0.2$ $P(b, v) \approx 0.2$.

220 The discrepancy between σ_d and σ_c is the result of the assumptions made in the Langevin model, where the capture is considered to be orientation-independent and the particles do not have any internal structure. If the anisotropy of the dipole–dipole potential is taken into account, as in Eq. (5), the capture cross section will be reduced (this has been estimated in Appendix A using a numerical approach provided by Maergoiz et al. (1996c)). However, if two molecules are able to move rather close to each other, translational energy can be transferred to rotational and vibrational modes, and therefore the motion over the centrifugal barrier is hindered, and the critical impact parameter effectively reduced. Additionally, steric hindrance caused by intermolecular orientations incompatible with the formation of hydrogen bonds will also lower the collision probability. Due to coupling, steric hindrance and other dynamical effects, the ratio between the cross sections σ_d and σ_c is on average 0.82 for the collision of two sulfuric acid molecules.

230 The canonical collision rate coefficient can be calculated similarly as Eq. (1), but since the collision probabilities $P(b^2)$ $P(b, v)$ obtained from the atomistic simulations depend on both the velocity and the impact parameter, the MD based collision

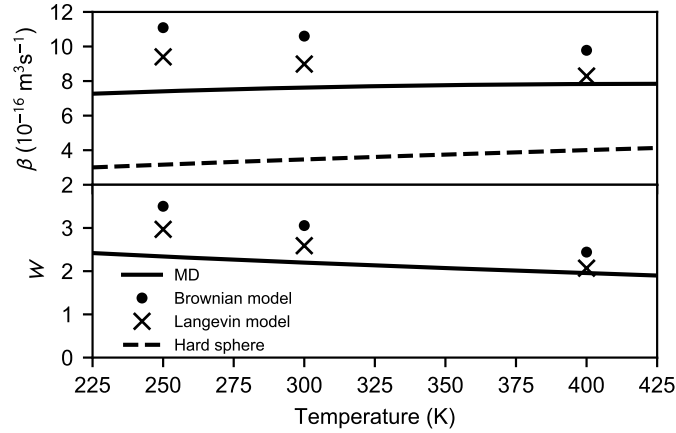


Figure 7. Collision rate coefficient β (upper panel) and the enhancement factor W (lower panel) as a function of temperature calculated for the hard-sphere, MD, Langevin and Brownian approaches.

rate coefficient is calculated by integrating over both the relative velocity distribution $f(v)$ and b^2 as

$$\beta_{\text{MD}} = \pi \int_0^{\infty} dv \int_0^{\infty} db^2 v f(v) P(b^2, v). \quad (13)$$

235 While the thermal velocity distribution $f(v)$ of the colliding molecules can be altered freely to correspond with an arbitrary temperature, the effect of the internal motion to the collision probability function is not necessarily temperature-invariant. However, in Appendix B it has been shown that a moderate change (simulations carried out at 250 and 400 K) in the internal kinetic energy does not effect the collision probabilities significantly. We therefore used the collision probability distributions calculated at 300 K to compute the collision rate coefficients for the atmospherically relevant temperature range $T = 225 - 425$ K (see Fig. 7).

In case of the Langevin model (Eq. (9)) the expression for the canonical capture rate coefficient can be simplified to

$$240 \quad \beta_{\text{L}} = \pi \int_0^{\infty} dv v f(v) b_c^2(v). \quad (14)$$

Since the potential of mean force is required for the Langevin model, the coefficients are calculated only at 250, 300 and 400 K (see Appendix B for further details).

245 ~~Instead of absolute values of the coefficients~~ In addition to the coefficients obtained by different approaches, we focus on examine the enhancement factor W relative to the kinetic gas theory rate expressed in Eq. (1), where a hard-sphere radius $R = 2.76 \text{ \AA}$ was calculated from the bulk liquid density of sulfuric acid, $\rho = 1830 \text{ kgm}^{-3}$, assuming a volume fraction of one. Therefore Thus, after performing the integration, the enhancement factor obtained using the Langevin model can be

expressed analytically as

$$W_L = \frac{\beta_L}{\beta_{HS}} = \frac{\pi}{\sqrt{3}\Gamma(\frac{1}{3})} \Gamma\left(\frac{16\epsilon}{k_B T} \frac{2}{3}\right) \left(\frac{2\epsilon}{k_B T}\right)^{1/3} \left(\frac{r_0}{2R}\right)^2, \quad (15)$$

where $\Gamma(x)$ denotes the Gamma function, and ϵ and r_0 are the parameters ~~from the fit to the attractive part of the~~ based on the potential of mean force between two sulfuric acid molecules in vacuum, using the functional form in Eq. (8). The enhancement factor from the Brownian model of aerosol coagulation, W_B , was calculated analytically from Eq. (10).

We find that $W_{MD} \approx 2.2$, $W_L \approx 2.64$, and $W_B \approx 3.11$. $W_{MD} \approx 2.20$, $W_L \approx 2.59$, and $W_B \approx 3.06$ at 300 K. ~~The enhancement factor obtained~~ Both the collision rate coefficients and the enhancement factors are shown in Fig. 7. As the hard-sphere collision rate is linearly increasing as the molecular velocity is proportional to \sqrt{T} , the rate coefficient based on atomistic simulations is only slightly increasing with temperature due to the exponential narrowing of the collision cross section as the relative velocity increases. However, the dependency is different in case of the Langevin model as the rate coefficient is decreasing with increasing temperature. This is due to the neglect of the anisotropy of the dipole-dipole interactions in the Langevin model: at higher temperatures, the effect of anisotropy becomes less important and therefore the model overestimates the collision rate less, compared to lower temperatures. The same effect can be observed in the Brownian coagulation model. Indeed, as seen from Fig. 7, the enhancement factors based on the theoretical models reach better agreement with the factor obtained from atomistic simulations as the temperature rises. As a result of the above-mentioned reasons, the enhancement factor over the hard-sphere collision rate coefficient is lower at higher temperatures regardless of the chosen approach.

The enhancement factor obtained by atomistic simulations is in very good agreement with the kinetic modelling on recent experimental results of formation of atmospheric sulfuric acid dimers (Kürten et al., 2014) and small clusters of sulfuric acid, dimethylamine and water (Lehtipalo et al., 2016; Kürten et al., 2018). In these studies, the enhancement factor was estimated to be 2.3–2.7 using the Brownian coagulation model and Van der Waals interactions fitted to experiment, as mentioned earlier, whereas according to our molecular model of long-range interaction the basic Brownian model using ~~a fit to~~ the attractive part of the potential of mean force overestimates the rate enhancement factor by ~~over~~ about 40 %.

4 Conclusions

In summary, we have benchmarked two classical force fields against experimental and ab initio data and determined that the OPLS force field by Loukonen et al. was able to describe the geometry and vibrational spectra of the isolated sulfuric acid molecule, as well as the geometry and binding free energy of the sulfuric acid dimer. We studied the statistics of collisions of sulfuric acid molecules in vacuum by molecular dynamics simulations and compared our results against simple theoretical models. We have found that the effective collision cross section of two H_2SO_4 molecules, as described by the OPLS force field, is significantly larger than the hard-sphere diameter assigned to the molecule based on the liquid density of sulfuric acid. As a consequence, we find the collision coefficient for sulfuric acid molecules is enhanced by a factor 2.2, compared to kinetic gas theory at 300 K. This enhancement factor obtained from atomistic simulation is consistent with the discrepancy observed

between experimental formation rates of clusters containing sulfuric acid and rates calculated using hard sphere kinetics. At a temperature range from 250 to 400 K, the rate enhancement factor is monotonously decreasing with increasing temperature, however the drop is less than 20 %. The velocity dependence of the simulated dynamical collision cross section is in good agreement with the Langevin model solution. We also note that the enhancement factor obtained from the Langevin model using ~~a fit to~~ the attractive part of the intermolecular potential is ~~within 20~~ a bit overestimated due to the imperfect treatment of the dipole-dipole interaction, yet in the atmospherically relevant temperature range the factor is within 30 % of the result from the atomistic simulation, at a fraction of the computational cost.

In the future, the atomistic collision modelling approach presented in this work can be applied to other atmospherically relevant molecules, clusters, or ions, exhibiting dipoles of varying magnitude – and in some cases several times larger than the one of the sulfuric acid molecule – to help understand the effect of long-range interactions in cluster formation rates. However, before we can quantitatively assess the influence of collision rate enhancement on atmospherical new particle formation rates obtained from cluster dynamics models (for example ACDC (McGrath et al., 2012)), it is necessary to obtain the enhancement factors for all the relevant collisions between clusters of different sizes and composition, as the pathway for growth may change – a formidable task, even if only the simplest acid-base clusters were considered. Future work therefore should also be aimed at finding simple models for predicting approximate rate enhancements, based on just a few physico-chemical properties, such as molecular structures, dipole moments or charge distributions, of the interacting molecules and/or clusters.

Appendix A: Effect of anisotropy on the dipole–dipole capture rate

Maergoiz et al. (1996c), using classical trajectory integration, calculated the capture rate constant when two identical polar molecules interact through a potential containing anisotropic ($\propto r^{-3}$) and isotropic ($\propto r^{-6}$) terms,

$$V = \frac{(\mathbf{d}_1 \cdot \mathbf{d}_2) - 3(\mathbf{d}_1 \cdot \mathbf{n})(\mathbf{d}_2 \cdot \mathbf{n})}{r^3} - \frac{C}{r^6}, \quad (\text{A1})$$

where \mathbf{d}_1 and \mathbf{d}_2 are the dipole moments vectors of the molecules, \mathbf{n} is the unit vector along the distance vector \mathbf{r} connecting the centres of mass of the molecules and C is the isotropic interaction constant.

As in Eq. (1), the capture rate coefficient in an anisotropic field is given by

$$\beta_{\text{aniso}} = \sqrt{\frac{8k_B T}{\pi\mu}} \bar{\sigma}_{\text{aniso}}, \quad (\text{A2})$$

where the thermal capture cross section can be calculated using a fitting function $\kappa(\theta, M)$ as

$$\bar{\sigma}_{\text{aniso}} = \pi \left(\frac{d^2}{k_B T} \right)^{2/3} \theta^{1/6} \kappa(\theta, M), \quad (\text{A3})$$

where d is the molecular dipole moment (for the OPLS model of sulfuric acid, $d = |\mathbf{d}_1| = |\mathbf{d}_2| = 3.07$ Debye). Maergoiz et al. use two dimensionless parameters in their model:

$$\theta = \frac{Ck_B T}{d^4}, \quad (\text{A4})$$

and

$$M = \frac{\mu d^{4/3}}{2I(k_B T)^{2/3}}. \quad (\text{A5})$$

Based on our MD simulations using the OPLS force field, the average moment of inertia I of a vibrating sulfuric acid molecule is 100.04 amuÅ², which deviates slightly from values 100.66 and 104.94 amuÅ² obtained experimentally (Kuczkowski et al., 1981) and from quantum chemical calculations (Zapadinsky et al., 2019), respectively. The fitting function is obtained from classical trajectory calculations and it is expressed as

$$\ln \kappa(\theta, M) = a_0 + \left(\frac{a_1^2 z}{\sinh(z)} + \frac{z^2}{36} \right)^{1/2}, \quad (\text{A6})$$

where

$$z = a_2 + \ln \theta. \quad (\text{A7})$$

The reported fitting parameters are (Maergoiz et al., 1996c)

$$a_0 = 0.2406 - 0.1596 (1 + 1.9192M^{0.9935})^{-1}, \quad (\text{A8a})$$

$$a_1 = 0.253 - 0.04573 (1 + 1.1645M^{0.6422})^{-1}, \quad (\text{A8b})$$

$$a_2 = 1.7617 + 0.9577 (1 + 1.9192M^{0.9935})^{-1}. \quad (\text{A8c})$$

Since all different long-range interactions are included in the attractive part of the potential of mean force between two sulfuric acid molecules (Eq. (8)), to exclude the dipole–dipole interaction from the isotropic interaction, the constant C is written as

$$C = (1 - f)\epsilon r_0^6, \quad (\text{A9})$$

where f is a factor denoting the relative magnitude of the anisotropic interaction between permanent dipoles with respect to the total interaction, and $\epsilon = 0.57$ eV and $r_0 = 4.1$ Å. Thus, the rate coefficient is controlled by the relative dipole–dipole interaction and the enhancement factor over the kinetic gas theory can be written as

$$W_{\text{aniso}}(f) = \frac{\beta_{\text{aniso}}(f)}{\beta_{\text{HS}}} = \frac{\bar{\sigma}_{\text{aniso}}(f)}{\pi(2R)^2}. \quad (\text{A10})$$

Figure A-A1 shows the rate enhancement as a function of the interaction factor f at 300 K. As the anisotropic part does not contribute, i.e. $f = 0$, the enhancement factor is only 3 less than 4 % higher than the value obtained from the Langevin model (the statistical error of the thermal capture cross section is about 2 % (Maergoiz et al., 1996c)).

Since we are unable to distinguish the actual dipole–dipole interaction from the total attractive potential, we have estimated the interaction using the Keesom equation (see Fig. 3):

$$U_K = \frac{2d^4}{3k_B T r^6} - \frac{d^4}{24\pi^2 \epsilon_0^2 k_B T r^6}. \quad (\text{A11})$$

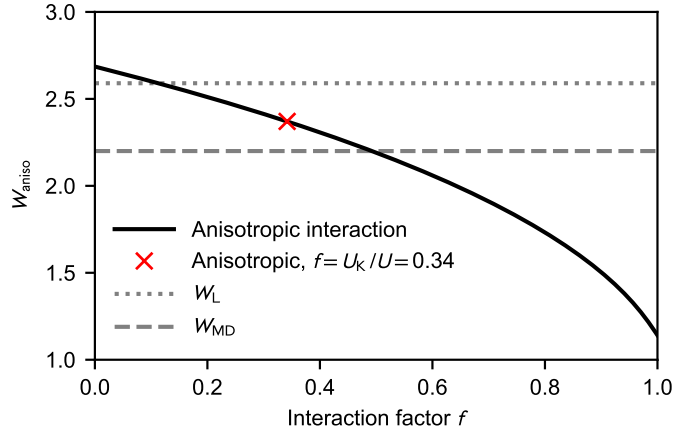


Figure A1. Enhancement factor W_{aniso} over the kinetic gas theory calculated from the anisotropic dipole–dipole collision cross section as a function of the interaction factor f at 300 K (black solid line). The red cross denotes the case where the dipole–dipole contribution of the total interaction equals the Keesom equation Eq. (A11) ($W_{\text{aniso}} = 2.41$). The enhancement factors obtained from the Langevin model and the MD simulations are shown as the dotted and dashed grey lines, respectively.

Table A1. The attractive potential parameters ϵ and r_0 for $\text{H}_2\text{SO}_4\text{--H}_2\text{SO}_4$ interaction based on the PMF calculations with the estimated anisotropic interaction factor $f = U_K/U$ and the corresponding enhancement factors calculated by the Langevin model W_L , anisotropic approach $W_{\text{aniso}}(f)$ and atomistic simulations W_{MD} .

T (K)	ϵ (eV)	r_0 (Å)	f	W_L	$W_{\text{aniso}}(f)$	W_{MD}
250	0.69	4.1	0.33	2.97	2.73	2.34
300	0.55	4.1	0.34	2.59	2.37	2.20
400	0.37	4.1	0.38	2.07	1.87	1.95

According to Eqs. (8) and (A11), about one third of the attractive potential is due to dipole–dipole interaction at 300 K, and consequently the enhancement factor is $W_{\text{aniso}} = 2.41$, lower than for the isotropic field. The estimated rate enhancement factors at 250, 300 and 400 K are shown in Tab. A1. Thus, by taking into account the anisotropy of the intermolecular potential, the estimated capture rate is in better agreement with the result obtained using atomistic simulation ($W_{\text{MD}} \approx 2.2$) than with the isotropic Langevin model ($W_L \approx 2.64$) as illustrated in Fig. A1 simulations.

Appendix B: Temperature dependence of collision probabilities and interaction parameters

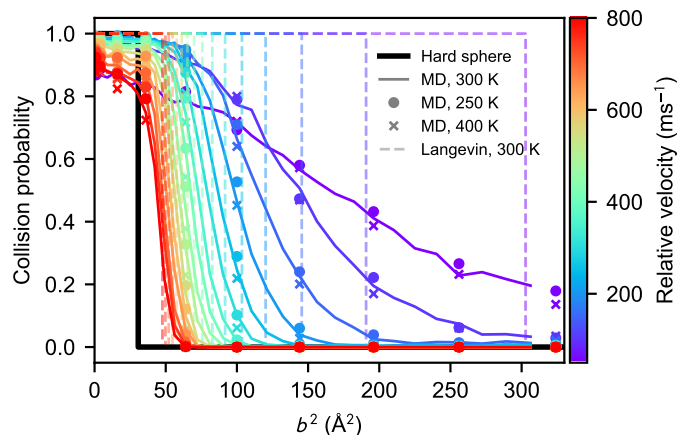


Figure B1. Collision probabilities of sulfuric acid molecules, as a function of the impact parameter squared, for different values of the relative velocity, obtained from molecular dynamics simulation at 300 K (solid coloured lines), at 250 K (coloured dots) and at 400 K (coloured crosses). The step-like collision probabilities for a hard-sphere model ($b^2 = (2R)^2$), or obtained from the Langevin capture model (Eq. (9)), are indicated by the solid black, and dashed coloured lines, respectively.

340 The canonical collision rate coefficient can be calculated from the collision probabilities obtained from atomistic simulation at arbitrary temperatures by shifting the Maxwell-Boltzmann relative velocity distribution, provided that changes in the internal motion of the molecules do not affect the collision probabilities. We have tested the effect of the different rotational and vibrational motion on the collision statistics in an atmospherically relevant temperature range by carrying out MD collision simulations for a subset of impact parameters b where the molecules' atomistic velocities were drawn from Maxwell-Boltzmann distributions corresponding to 250 K and 400 K, instead of 300 K. As shown in Fig. B1, such moderate change in temperature indeed does not affect the collision probabilities between two sulfuric acid molecules.

In order to vary temperature in calculating the thermal collision rate coefficient using the Langevin approach, the potential of mean force between two sulfuric acid molecules was calculated at 250 K, 300 K, and 400 K, and the parameters describing the attractive intermolecular interaction (Eq. (8)) are reported in Table A1.

350 Appendix C: Intermolecular repulsion at low velocities in MD simulations

As shown in Fig. 5 and B1, for small values of the impact parameter and initial relative velocity between two colliding molecules in the atomistic simulations, the collision probability can be considerably smaller than unity, which seems counter-intuitive at first. This is due to the fact that the intermolecular interaction is anisotropic and the molecules are rotating, which can lead to instantaneous repulsion even at distances where the intermolecular potential of mean force is slightly attractive. If the initial translational kinetic energy is low enough, the temporary fluctuations in intermolecular energy can alter the translational motion and eventually lead to a definitive separation of the molecules.

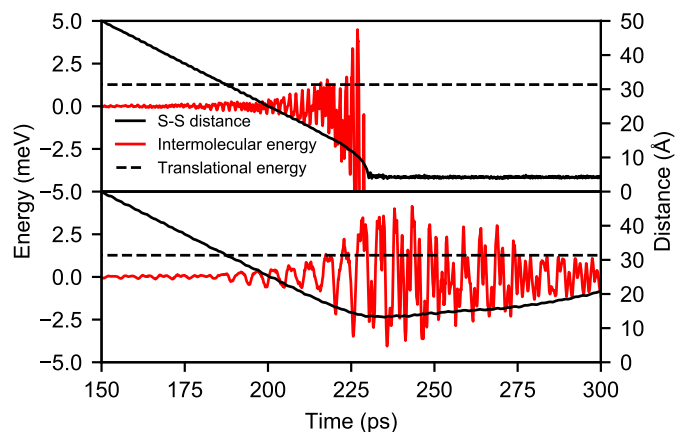


Figure C1. Time evolution of the intermolecular energy (red line) and the sulfur–sulfur distance (solid black line) in one MD trajectory with relative velocity $v = 50 \text{ ms}^{-1}$ and $b = 0 \text{ \AA}$ where a collision occurs (top) and one where the molecules are repelled at range (bottom). The initial translational kinetic energy of the molecules (1.27 meV) is indicated by the dashed black line.

This process is illustrated in Fig. C1, which shows the evolution of the intermolecular energy and distance in one trajectory with $b = 0 \text{ \AA}$ and $v = 50 \text{ ms}^{-1}$ where a collision occurs and a second one where the molecules are repelled at range. While in both cases the fluctuation of the intermolecular energy exceeds the initial translational energy of 1.27 meV, in the trajectory
 360 exhibiting a repulsion, the large positive energy fluctuations are longer lived and dominate the interaction.

Author contributions. RH and BR planned the simulation setup and performed benchmark calculations. BR carried out collision and metadynamics simulations and wrote the first draft of the paper. RH and EZ provided the theoretical framework. RH analyzed the simulation data. TK and HV helped plan the project and all authors contributed to writing the manuscript.

Competing interests. The authors declare that they have no conflict of interest.

365 *Acknowledgements.* This work was supported by the European Research Council (project 692891 DAMOCLES), Academy of Finland (Academy Research Fellow project 1266388 and ARKTIKO project 285067 ICINA), and University of Helsinki, Faculty of Science AT-MATH project. Computational resources were provided by CSC–IT Center for Science, Ltd., Finland.

References

- Almeida, J., Schobesberger, S., Kürten, A., Ortega, I. K., Kupiainen-Määttä, O., Praplan, A. P., Adamov, A., Amorim, A., Bianchi, F.,
370 Breitenlechner, M., et al.: Molecular understanding of sulphuric acid–amine particle nucleation in the atmosphere, *Nature*, 502, 359, 2013.
- Barducci, A., Bussi, G., and Parrinello, M.: Well-Tempered Metadynamics: A Smoothly Converging and Tunable Free-Energy Method, *Phys. Rev. Lett.*, 100, 020 603, 2008.
- Chackalackal, S. M. and Stafford, F. E.: Infrared Spectra of the Vapors above Sulfuric and Deuteriosulfuric Acids, *J. Am. Chem. Soc.*, 88,
375 723–728, 1966.
- Chan, T. W. and Mozurkewich, M.: Measurement of the coagulation rate constant for sulfuric acid particles as a function of particle size using tandem differential mobility analysis, *J. Aerosol Sci.*, 32, 321–339, 2001.
- Chesnavich, W. J., Su, T., and Bowers, M. T.: Collisions in a noncentral field: a variational and trajectory investigation of ion–dipole capture, *J. Chem. Phys.*, 72, 2641–2655, 1980.
- 380 Clary, D.: Calculations of rate constants for ion-molecule reactions using a combined capture and centrifugal sudden approximation, *Mol. Phys.*, 54, 605–618, 1985.
- Ding, C. G., Taskila, T., Laasonen, K., and Laaksonen, A.: Reliable potential for small sulfuric acid-water clusters, *Chem. Phys.*, 287, 7–19, 2003.
- Dugan Jr., J. V. and Magee, J. L.: Capture collisions between ions and polar molecules, *J. Chem. Phys.*, 47, 3103–3112, 1967.
- 385 Elm, J., Jen, C. N., Kurtén, T., and Vehkamäki, H.: Strong Hydrogen Bonded Molecular Interactions between Atmospheric Diamines and Sulfuric Acid, *J. Phys. Chem. A*, 120, 3693–3700, 2016.
- Hintze, P. E., Kjaergaard, H. G., Vaida, V., and Burkholder, J. B.: Vibrational and electronic spectroscopy of sulfuric acid vapor, *J. Phys. Chem. A*, 107, 1112–1118, 2003.
- Israelachvili, J. N.: *Intermolecular and Surfaces Forces*, Academic Press, 3rd edn., 2011.
- 390 Jorgensen, W. L., Maxwell, D. S., and Tirado-Rives, J.: Development and Testing of the OPLS All-Atom Force Field on Conformational Energetics and Properties of Organic Liquids, *J. Am. Chem. Soc.*, 118, 11 225–11 236, 1996.
- Kuczkowski, R. L., Suenram, R. D., and Lovas, F. J.: Microwave spectrum, structure, and dipole moment of sulfuric acid, *J. Am. Chem. Soc.*, 103, 2561–2566, 1981.
- Kürten, A., Jokinen, T., Simon, M., Sipilä, M., Sarnela, N., Junninen, H., Adamov, A., Almeida, J., Amorim, A., Bianchi, F.,
395 et al.: Neutral molecular cluster formation of sulfuric acid–dimethylamine observed in real time under atmospheric conditions, *Proc. Natl. Acad. Sci. USA*, 111, 15 019–15 024, 2014.
- Kürten, A., Li, C., Bianchi, F., Curtius, J., Dias, A., Donahue, N. M., Duplissy, J., Flagan, R. C., Hakala, J., Jokinen, T., Kirkby, J., Kulmala, M., Laaksonen, A., Lehtipalo, K., Makhmutov, V., Onnela, A., Rissanen, M. P., Simon, M., Sipilä, M., Stozhkov, Y., Tröstl, J., Ye, P., and McMurry, P. H.: New particle formation in the sulfuric acid–dimethylamine–water system: reevaluation of CLOUD chamber
400 measurements and comparison to an aerosol nucleation and growth model, *Atmos. Chem. Phys.*, 18, 845–863, 2018.
- Landau, L. D. and Lifshitz, E. M.: *Mechanics*, vol. 1, *Course of Theoretical Physics*, Butterworth-Heinemann, 3rd edn., 1976.
- Langevin, P.: A fundamental formula of kinetic theory, *Ann. Chim. Phys.*, 5, 245–288, 1905.
- Lehtipalo, K., Rondo, L., Kontkanen, J., Schobesberger, S., Jokinen, T., Sarnela, N., Kürten, A., Ehrhart, S., Franchin, A., Nieminen, T., et al.: The effect of acid–base clustering and ions on the growth of atmospheric nano-particles, *Nat. Commun.*, 7, 11 594, 2016.

- 405 Loukonen, V., Kurtén, T., Ortega, I. K., Vehkamäki, H., Pádua, A. A. H., Sellegri, K., and Kulmala, M.: Enhancing effect of dimethylamine in sulfuric acid nucleation in the presence of water – a computational study, *Atmos. Chem. Phys.*, 10, 4961–4974, 2010.
- Loukonen, V., Bork, N., and Vehkamäki, H.: From collisions to clusters: first steps of sulphuric acid nanocluster formation dynamics, *Mol. Phys.*, 112, 1979–1986, 2014.
- Maergoiz, A., Nikitin, E., Troe, J., and Ushakov, V.: Classical trajectory and adiabatic channel study of the transition from adiabatic to sudden capture dynamics. I. Ion–dipole capture, *J. Chem. Phys.*, 105, 6263–6269, 1996a.
- 410 Maergoiz, A., Nikitin, E., Troe, J., and Ushakov, V.: Classical trajectory and adiabatic channel study of the transition from adiabatic to sudden capture dynamics. II. Ion–quadrupole capture, *J. Chem. Phys.*, 105, 6270–6276, 1996b.
- Maergoiz, A., Nikitin, E., Troe, J., and Ushakov, V.: Classical trajectory and adiabatic channel study of the transition from adiabatic to sudden capture dynamics. III. Dipole–dipole capture, *J. Chem. Phys.*, 105, 6277–6284, 1996c.
- 415 Marlow, W. H.: Derivation of aerosol collision rates for singular attractive contact potentials, *J. Chem. Phys.*, 73, 6284–6287, 1980.
- McGrath, M. J., Olenius, T., Ortega, I. K., Loukonen, V., Paasonen, P., Kurtén, T., Kulmala, M., and Vehkamäki, H.: Atmospheric Cluster Dynamics Code: a flexible method for solution of the birth-death equations, *Atmos. Chem. Phys.*, 12, 2345–2355, 2012.
- Miller, Y., Chaban, G., and Gerber, R.: Ab Initio Vibrational Calculations for H_2SO_4 and $\text{H}_2\text{SO}_4 \cdot \text{H}_2\text{O}$: Spectroscopy and the Nature of the Anharmonic Couplings, *J. Phys. Chem. A*, 109, 6565–6574, 2005.
- 420 Moran, T. F. and Hamill, W. H.: Cross Sections of Ion—Permanent-Dipole Reactions by Mass Spectrometry, *J. Chem. Phys.*, 39, 1413–1422, 1963.
- Myllys, N., Olenius, T., Kurtén, T., Vehkamäki, H., Riipinen, I., and Elm, J.: Effect of Bisulfate, Ammonia, and Ammonium on the Clustering of Organic Acids and Sulfuric Acid, *J. Phys. Chem. A*, 121, 4812–4824, 2017.
- Napari, I., Vehkamäki, H., and Laasonen, K.: Molecular dynamic simulations of atom–cluster collision processes, *J. Chem. Phys.*, 120, 165–169, 2004.
- 425 Ouyang, H., Gopalakrishnan, R., and Hogan Jr, C. J.: Nanoparticle collisions in the gas phase in the presence of singular contact potentials, *J. Chem. Phys.*, 137, 064316, 2012.
- Pinchuk, A. O.: Size-dependent Hamaker constant for silver nanoparticles, *J. Phys. Chem. C*, 116, 20099–20102, 2012.
- Plimpton, S.: Fast Parallel Algorithms for Short-Range Molecular Dynamics, *J. Comp. Phys.*, 117, 1–19, 1995.
- 430 Sceats, M. G.: Brownian coagulation in a field of force, *J. Chem. Phys.*, 84, 5206–5208, 1986.
- Sceats, M. G.: Brownian coagulation in aerosols—the role of long range forces, *J. Colloid Interface Sci.*, 129, 105–112, 1989.
- Sedo, G., Schultz, J., and Leopold, K. R.: Electric dipole moment of sulfuric acid from Fourier transform microwave spectroscopy, *J. Mol. Spectrosc.*, 251, 4–8, 2008.
- Su, T. and Bowers, M. T.: Theory of ion–polar molecule collisions. Comparison with experimental charge transfer reactions of rare gas ions to geometric isomers of difluorobenzene and dichloroethylene, *J. Chem. Phys.*, 58, 3027–3037, 1973.
- 435 Su, T. and Chesnavich, W. J.: Parametrization of the ion–polar molecule collision rate constant by trajectory calculations, *J. Chem. Phys.*, 76, 5183–5185, 1982.
- Su, T., Su, E. C., and Bowers, M. T.: Ion–polar molecule collisions. Conservation of angular momentum in the average dipole orientation theory. The AADO theory, *J. Chem. Phys.*, 69, 2243–2250, 1978.
- 440 Temelso, B., Phan, T. N., and Shields, G. C.: Computational Study of the Hydration of Sulfuric Acid Dimers: Implications for Acid Dissociation and Aerosol Formation, *J. Phys. Chem. A*, 116, 9745–9758, 2012.

- Tribello, G. A., Bonomi, M., Branduardi, D., Camilloni, C., and Bussi, G.: Plumed 2: New feathers for an old bird, *Comput. Phys. Commun.*, 185, 604–613, 2014.
- Troe, J.: Statistical adiabatic channel model for ion–molecule capture processes, *J. Chem. Phys.*, 87, 2773–2780, 1987.
- 445 Yang, H., Goudeli, E., and Hogan Jr, C. J.: Condensation and dissociation rates for gas phase metal clusters from molecular dynamics trajectory calculations, *J. Chem. Phys.*, 148, 164 304, 2018.
- Zapadinsky, E., Passananti, M., Myllys, N., Kurtén, T., and Vehkamäki, H.: Modeling on Fragmentation of Clusters inside a Mass Spectrometer, *J. Phys. Chem. A*, 123, 611–624, 2019.